G. JUNAK*#

LOW-CYCLE FATIGUE CHARACTERISTICS OF SELECTED TITANIUM, MAGNESIUM AND ALUMINIUM ALLOYS

In the paper, on the basis of the performed tests, low-cycle fatigue characteristics (LCF) of selected light metal alloys used among others in the automotive and aviation industries were developed. The material for the research consisted of hot-worked rods made of magnesium alloy EN-MAMgAl3Zn1, two-phase titanium alloy Ti6Al4V and aluminium alloy AlCu4MgSi(A). Alloys used in components of means of transport should have satisfactory fatigue, including low-cycle fatigue, characteristics. Low-cycle fatigue tests were performed on an MTS-810 machine at room temperature. Low-cycle fatigue tests were performed for three total strain ranges $\Delta\varepsilon_t = 0.8\%$, 1.0% and 1.2% with a cycle asymmetry coefficient $R = -1$. On the basis of the obtained results, characteristics of the fatigue life of materials, cyclic deformation $\sigma_a = f(N)$ and cyclic deformation of the tested alloys were developed. The tests showed that titanium alloy Ti6Al4V was characterised by the highest fatigue life N_f, whereas the lowest fatigue life was found in the tests of the aluminium alloy AlCu4MgSi(A).

Keywords: fatigue life, low-cycle fatigue, light metal alloys

1. Introduction

Light metal alloys which can be deformed by means of plastic working, such as titanium alloy Ti6Al4V, aluminium alloy AlCu4MgSi(A) and magnesium alloy EN-MAMgAl3Zn1 are increasingly used in the automotive, machine building, railway and aviation industries [1÷4]. The growing interest in alloys based on light metals for applications in the automotive and aviation industries is caused primarily by the drive to reduce vehicle weight and fuel consumption.

Precipitation strengthened two-phase titanium alloy Ti6Al4V is often used because of its good relationship between strength and ductile properties. The increase in tensile strength with the simultaneous decrease in plastic properties is achieved by the application of solution-heat and aging processes [5,6]. In addition, it is used in the aviation and chemical industries [1]. For example, alloy Ti6Al4V is used in the aviation industry for frames, wing leading edges, hydraulic and pneumatic conduits, landing flaps, etc. [5]. It is also used for hollow stepped axles and shafts in the machine and railway industries [2].

On the other hand, magnesium alloy EN-MAMgAl3Zn1 has good mechanical properties and is not too expensive. It can be shaped by processes such as rolling, extrusion and forging [7]. Its low density makes it an attractive material for the automotive industry [3,4]. The use of wrought magnesium alloys was sporadic, which was a result of technological difficulties in plastic processing and high manufacturing costs. The low

deformability of magnesium alloys at temperatures up to 200°C was caused by a limited number of slip systems in the hexagonal crystal network [8÷11]. Therefore, the number of alloy grades used for plastic processing is significantly lower than that of casting alloys. The mechanical properties of magnesium alloys after plastic processing are higher than those of cast alloys [4]. Alloys from the Mg-Al-Zn-Mn group, which contain up to 8% of Al with the addition of Mn (up to 2%) and Zn (up to 1.5%) [1,12,13], have the most favourable set of properties.

Aluminium alloy AlCu4MgSi(A) is very susceptible to pressing and bending. This alloy is moderately resistant to corrosion, but it is used, among others due to its good strength properties, in the production of components for the automotive industry, machine building parts and structural elements of aircraft [1]. Aluminium alloy AlCu4MgSi(A) is mainly used in the automotive and aviation industries [1,14]. It is estimated that over 60% of aircraft structures are made of aluminium alloys [1].

The usefulness of the above mentioned wrought alloys for applications as structural elements is determined not only by their low density, but also by a number of favourable mechanical properties UTS(R_m), YS($R_{p0.2}$), A. Moreover, light metal alloys wrought into equipment components for use in the automotive and aviation industries should have favourable fatigue characteristics [15].

Taking this into account, fatigue tests of this group of light metal alloys were carried out in the paper. Low-cycle fatigue

* SILESIAN UNIVERSITY OF TECHNOLOGY, INSTITUTE OF MATERIALS ENGINEERING, 8 KRASIŃSKIEGO STR., 40-019 KATOWICE, POLAND

\# Corresponding author: grzegorz.junak@polsl.pl

tests were performed at room temperature with a cycle asymmetry coefficient $R = -1$. Low-cycle fatigue tests were carried out on an MTS-810 machine with three total deflection ranges o $\Delta\varepsilon_t = 0.8\%$, 1.0% and 1.2%. On the basis of the obtained results, fatigue characteristics were developed, which can be used in predicting the durability of equipment elements made of the above-mentioned group of materials.

2. Research material

The material for the research consisted of hot-worked rods made of alloy EN-MAMgAl3Zn1, two-phase titanium alloy Ti6Al4V and aluminium alloy AlCu4MgSi(A). After extrusion, magnesium alloy rods with a diameter of 12 mm were annealed at 400ºC with the soaking time of 60 minutes and then cooled in the air. The main mechanical properties of the materials tested at room temperature determined on the basis of a static tensile test (Fig. 1) are presented in Table 1. The characteristic feature of the magnesium alloy in comparison with other materials was the lower value of proof stress YS($R_{p0.2}$) determined in static compression test conditions compared to the one determined in the tensile test, Fig. 2.
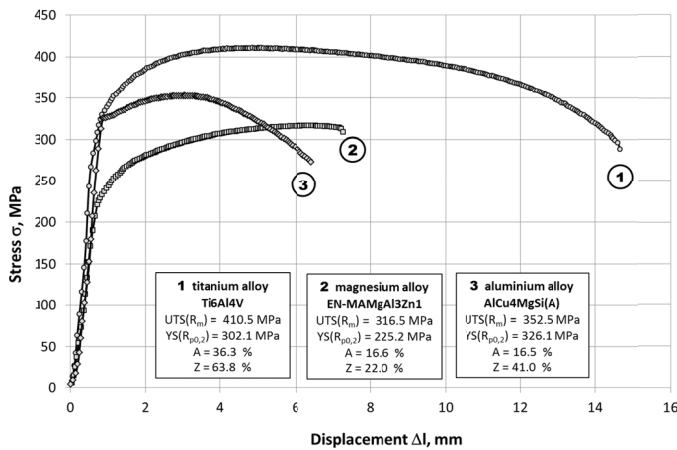

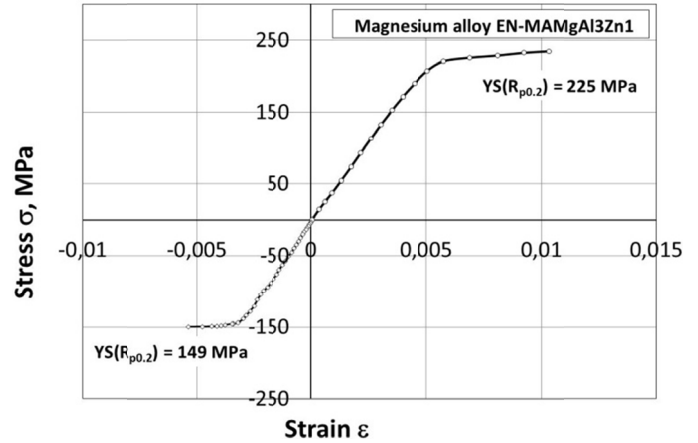Fig. 1. Diagrams of static tensile tests of tested alloys

Fig. 2. Diagram of static tensile and compression test of magnesium alloy EN-MAMgAl3Zn1

TABLE 1

Main mechanical properties of the selected light metal alloys

| Alloy | Main mechanical properties | | | | |
	UTS(R_m), MPa	YS($R_{p0.2}$), MPa	A, %	Z, %	E, GPa
EN-MAMgAl3Zn1	316.5	225.2	16.6	22.0	43.7
AlCu4MgSi(A)	352.5	326.1	16.5	41.0	75.1
Ti6Al4V	410.5	302.1	36.3	63.8	101.2

3. Research methodology and results

Low-cycle fatigue tests were performed on an MTS-810 strength testing machine. Screwed cylindrical specimens with a diameter of 12 mm were used in the tests. Fatigue tests were performed in tension and compression conditions with a cycle asymmetry coefficient $R = -1$. The tests were performed with the machine controlled by strain for three total strain ranges $\Delta\varepsilon_t = 0.8\%$, 1.0% and 1.2%. During the tests, hysteresis loops characteristic for the fatigue process stage, corresponding to a half of the number of cycles to fracture, were recorded (Figs. 3÷5).

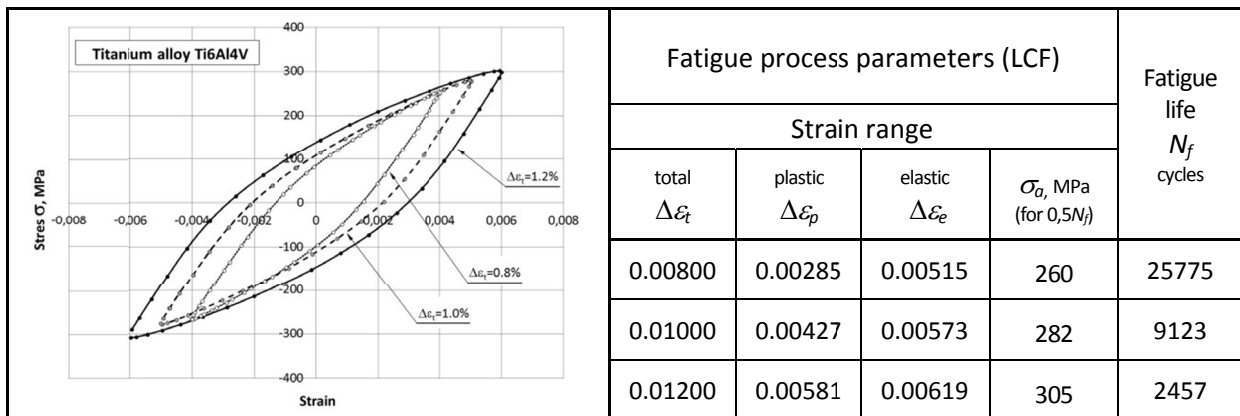| Fatigue process parameters (LCF) | | | | Fatigue life N_f cycles |
| Strain range | | | | |
total $\Delta\varepsilon_t$	plastic $\Delta\varepsilon_p$	elastic $\Delta\varepsilon_e$	σ_a, MPa (for 0,5N_f)	
0.00800	0.00285	0.00515	260	25775
0.01000	0.00427	0.00573	282	9123
0.01200	0.00581	0.00619	305	2457

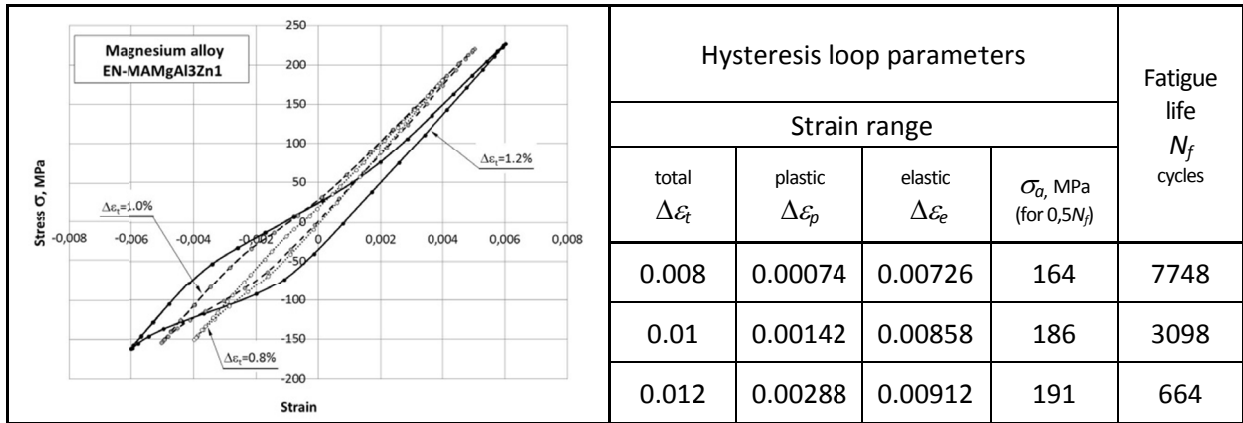Fig. 3. Hysteresis loops parameters determined for a half of the number of cycles to failure of titanium alloy Ti6Al4V

Fig. 4. Hysteresis loops parameters determined for a half of the number of cycles to failure of magnesium alloy EN-MAMgAl3Zn1
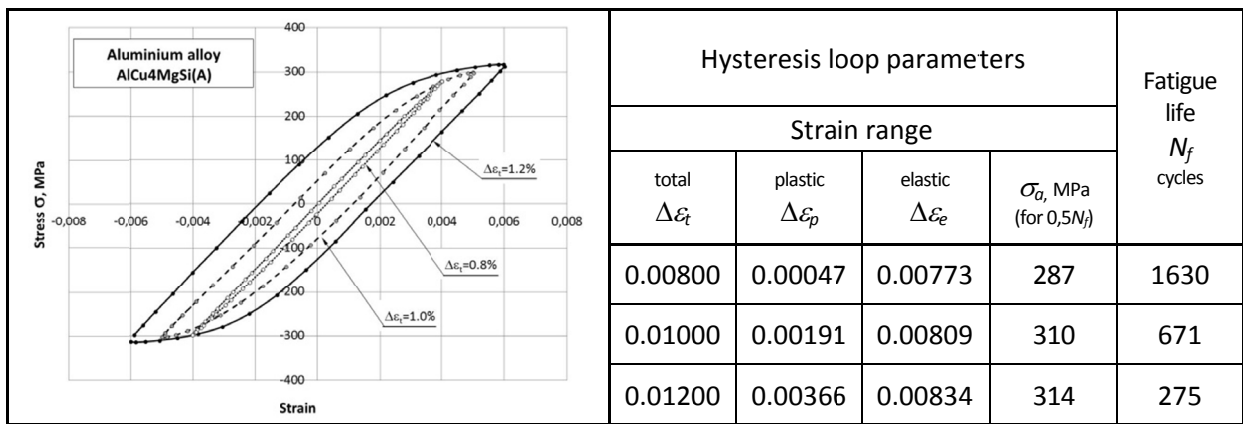
Hysteresis loop parameters				Fatigue life N_f cycles
Strain range				
total $\Delta\varepsilon_t$	plastic $\Delta\varepsilon_p$	elastic $\Delta\varepsilon_e$	σ_a, MPa (for 0,5N_f)	
0.008	0.00074	0.00726	164	7748
0.01	0.00142	0.00858	186	3098
0.012	0.00288	0.00912	191	664

Fig. 5. Hysteresis loops parameters determined for a half of the number of cycles to failure of aluminium alloy AlCu4MgSi(A)

Hysteresis loop parameters				Fatigue life N_f cycles
Strain range				
total $\Delta\varepsilon_t$	plastic $\Delta\varepsilon_p$	elastic $\Delta\varepsilon_e$	σ_a, MPa (for 0,5N_f)	
0.00800	0.00047	0.00773	287	1630
0.01000	0.00191	0.00809	310	671
0.01200	0.00366	0.00834	314	275

On the basis of the performed tests, the characteristics of low-cycle life (1) were developed as in Figs. 6÷7.

$$N_f = f(\Delta\varepsilon_t) \qquad (1)$$

where:

N_f – the number of cycles to fracture,
$\Delta\varepsilon_t$ – total strain range.

Diagrams of cyclic material deformation (2), shown in Figs. 8÷10, have also been developed.

$$\sigma_a = f(N) \qquad (2)$$

where:

σ_a – amplitude stress determined for a half of the number of cycles to fracture,
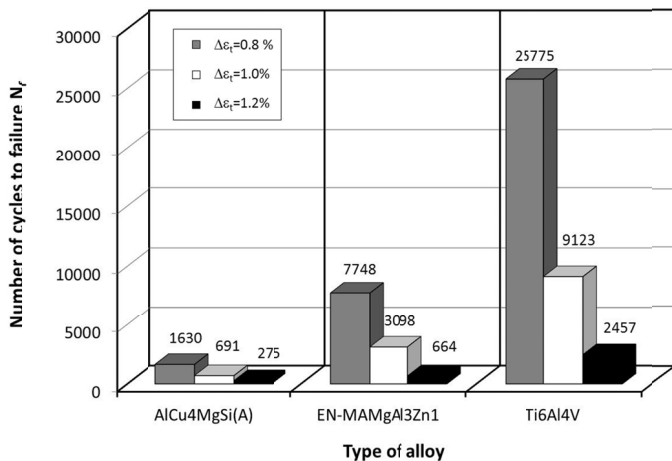N – the number of cycles.

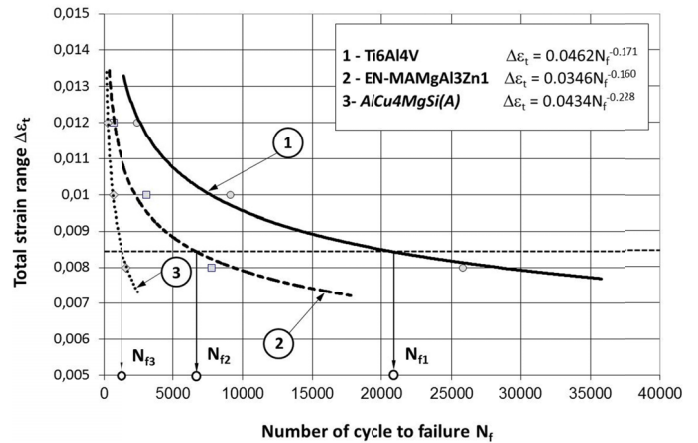Fig. 6. Characteristics of fatigue life of the tested alloys

Fig. 7. Characteristics of fatigue life of the tested alloys in the form of dependence $N_f = f(\Delta\varepsilon_t)$
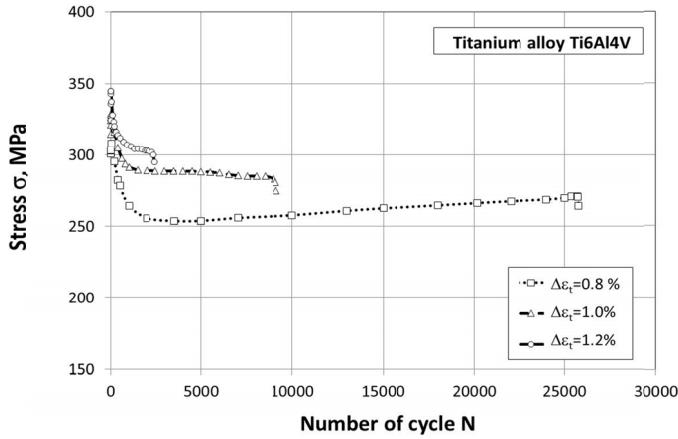
Fig. 8. Characteristics of cyclic deformation of titanium alloy Ti6Al4V
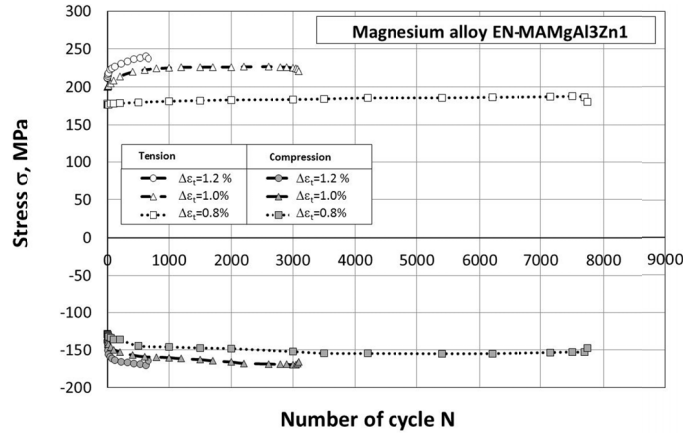

Fig. 9. Characteristics of cyclic deformation of magnesium alloy EN-MAMgAl3Zn1
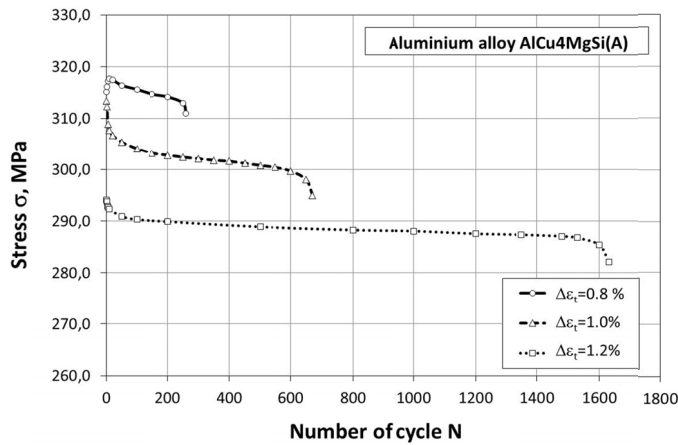

Fig. 10. Characteristics of cyclic deformation of aluminium alloy AlCu4MgSi(A)
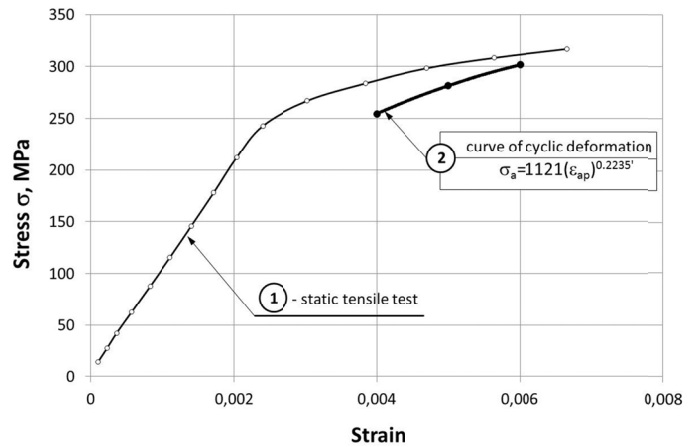

Fig. 11. Characteristics of cyclic deformation of titanium alloy Ti6Al4V against the background of the static tensile test diagram
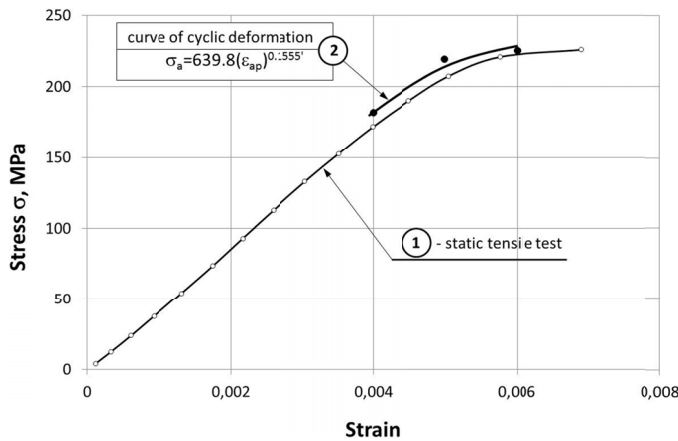

Fig. 12. Characteristics of cyclic deformation of magnesium alloy EN-MAMgAl3Zn1 against the background of the static tensile test diagram
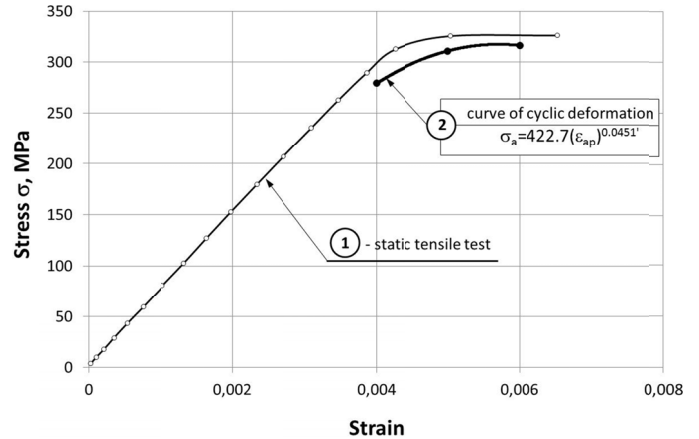

Fig. 13. Characteristics of cyclic deformation of aluminium alloy AlCu4MgSi(A) against the background of the static tensile test diagram

The obtained results were used to develop cyclic deformation diagrams (3) shown in Figs. 11÷13, [16].

$$\sigma_a = K'(\varepsilon_{apl})^{n'} \qquad (3)$$

where:

K' – cyclic strength coefficient,
n' – cyclic strengthening exponent.

On the basis of the characteristic parameters of the process of low-cycle fatigue of the tested alloys listed in the tables in Figures 3÷5, fatigue life characteristics (4) were developed in the form provided by Morrow [16÷18].

$$\varepsilon_{at} = \varepsilon_{ae} + \varepsilon_{ap} = \frac{\sigma'_f}{E}\left(2N_f\right)^b + \varepsilon'_f\left(2N_f\right)^c \qquad (4)$$
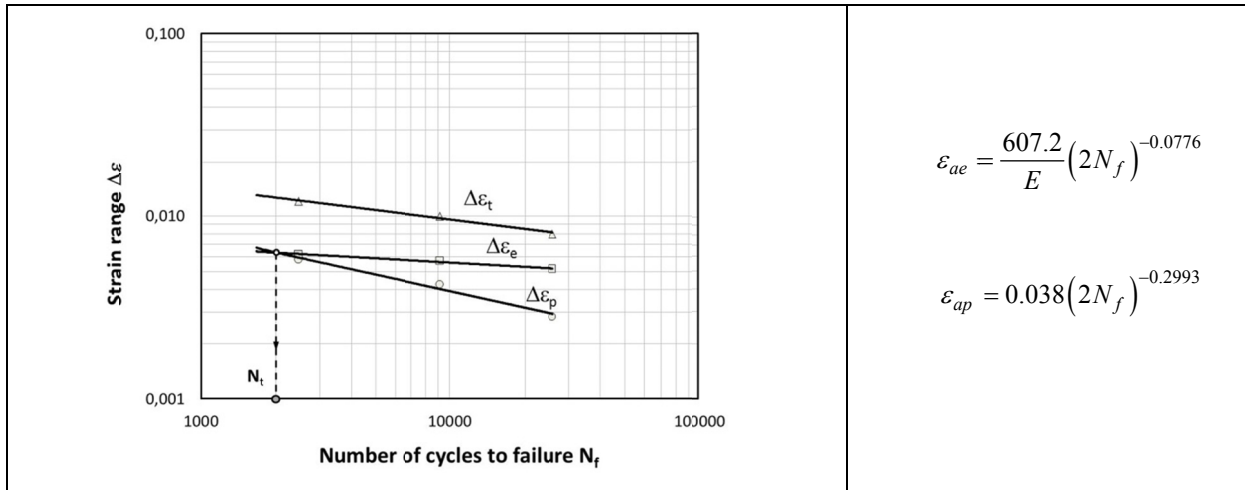
Fig. 14. Characteristics of fatigue life of titanium alloy Ti6Al4V

$$\varepsilon_{ae} = \frac{607.2}{E}\left(2N_f\right)^{-0.0776}$$

$$\varepsilon_{ap} = 0.038\left(2N_f\right)^{-0.2993}$$
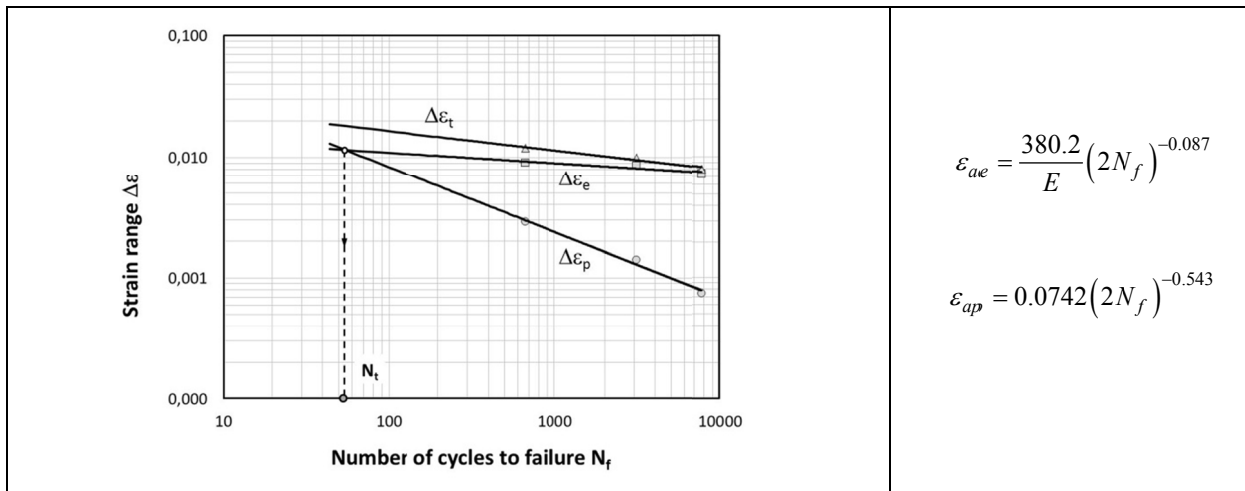
Fig. 15. Characteristics of fatigue life of magnesium alloy EN-MAMgAl3Zn1

$$\varepsilon_{ae} = \frac{380.2}{E}\left(2N_f\right)^{-0.087}$$

$$\varepsilon_{ap} = 0.0742\left(2N_f\right)^{-0.543}$$
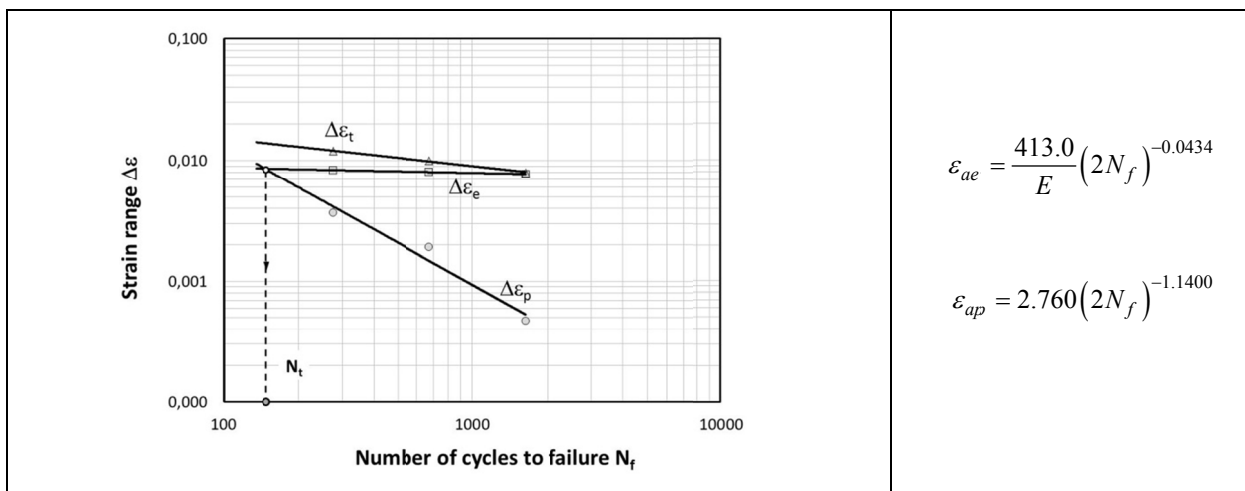
Fig. 16. Characteristics of fatigue life of aluminium alloy AlCu4MgSi(A)

$$\varepsilon_{ae} = \frac{413.0}{E}\left(2N_f\right)^{-0.0434}$$

$$\varepsilon_{ap} = 2.760\left(2N_f\right)^{-1.1400}$$

where:
$2N_f$ – the number of load reversals (half cycles),
σ_f' – fatigue strength coefficient,
ε_f' – fatigue ductility coefficient,

b – fatigue strength exponent,
c – fatigue ductility exponent.

Parameters characterising the process of low-cycle fatigue of the examined alloys are listed in Table 2.

TABLE 2

List of parameters used to describe the low-cycle fatigue process

Alloy	Parameter value					
	Fatigue strength coefficient	Fatigue strength exponent	Fatigue ductility coefficient	Fatigue ductility exponent	cyclic strength coefficient	cyclic strain hardening exponent
	σ'_f, MPa	b, -	ε'_f, mm/mm	c, -	K', MPa	n', -
Ti6Al4V	607.2	−0.0776	0.0380	−0.2993	1121	0.2235
EN-MAMgAl3Zn1	380.2	−0.0870	0.0742	−0.5430	639.8	0.1555
AlCu4MgSi(A)	413.0	−0.0434	2.76	−1.14	422.7	0.0451

4. Analysis of research results

The analysis of the results of the static tensile test (Table 1) has shown that the best strength UTS(R_m), YS($R_{p0.2}$) and ductile properties (A) are present in titanium alloy Ti6Al4V, for which UTS(R_m) = 410 MPa, YS($R_{p0.2}$) = 302 MPa, A_5 = 36%. The mechanical properties of the aluminium alloy were at a level of UTS(R_m) = 316 MPa, YS($R_{p0.2}$) = 225 MPa, A_5 = 16.6%. On the other hand, magnesium alloy EN-MAMgAl3Zn1 had the lowest mechanical properties UTS(R_m) = 316 MPa, YS($R_{p0.2}$) = 225 MPa, A = 16.5%.

In the performed tests the process of low-cycle fatigue of the tested alloys occurred with a dominant participation of the elastic component ($\Delta\varepsilon_e$) of the total strain range ($\Delta\varepsilon_t$), i.e. above point N_t (as shown in Figs. 14÷16). The highest shares of the plastic strain range ($\Delta\varepsilon_p$ – the widest hysteresis loops) were observed in the tests of titanium alloy Ti6Al4V. Despite this, the alloy showed the highest ability to transmit elastic-plastic deformations, expressed as the number of cycles to fracture N_f (Figs. 3÷5). EN-MAMgAl3Zn1 magnesium alloy showed significantly lower durability and the lowest durability was found in aluminium alloy AlCu4MgSi(A) (Figs. 6÷7).

Very unusual behaviour of magnesium alloy EN-MAMgAl3Zn1 was observed during the tests. The recorded loops were characterized by unexpected changes and anomalies of shape, already described in the literature [17], especially in the area of compressive stress (Fig. 4). As it is shown in literature [1] such a phenomenon usually occurs when elongation and rotation of individual grains happen during hard plastic processing. Such alloys are characterised by anisotropic behaviour regarding tensile and compressive stress what is defined as *strength differential effect* – SDE.

Furthermore, during the process of low-cycle fatigue of this group of alloys, significant differences in the surface of the hysteresis loop were observed (Figs. 3÷5). No relationship was found here between the size of the area of this surface (corresponding to the destruction energy accumulated in the specimen in each cycle) and low-cycle life N_f of a given alloy. The durability of titanium alloy for which hysteresis loops were the widest was the highest for the relevant total strain ranges ($\Delta\varepsilon_t$) and exceeded the durability of the magnesium alloy as well as the aluminium alloy, which demonstrated the lowest durability (Figs. 6÷7). The distortion of the hysteresis loop observed in magnesium alloy tests (Fig. 4), and the lack of symmetry between tension and compression half-cycles could have been caused by a different value $R_{p0.2}$ determined in static tensile and compression test conditions.

Under fatigue test conditions aluminium alloy AlCu4MgSi(A) and titanium alloy Ti6Al4V were characterised by cyclic weakening (Figs. 8 and 10). On the other hand, the magnesium alloy showed cyclic strengthening (Fig. 9). This is corroborated by the position of the cyclic deformation characteristics in relation to the static tensile characteristics (Figs. 11÷13). This is because the characteristics of cyclic deformation of titanium and aluminium alloys are below the static tensile diagram, which indicates weakening of the materials. In the case of magnesium alloy, however, the cyclic deformation characteristics are above the static tensile characteristics, which results in strengthening of the material [16].

5. Conclusions

1. In the LCF tests the longest fatigue life was observed for titanium alloy Ti6Al4V and the shortest for aluminium alloy AlCu4MgSi(A).
2. Titanium and aluminium alloys were characterised in the low-cycle fatigue test by cyclic weakening, whereas the magnesium alloy was characterised by cyclic strengthening.
3. The analyzed alloys did not show state of saturation during LCF tests.
4. Hysteresis loops observed in the process of low-cycle fatigue of magnesium alloy EN-MAMgAl3Zn1 showed anomalies of shape.

REFERENCES

[1] K. E. Oczoś, A. Kawalec, Forming Light Metals, PWN, Warsaw (2012).

[2] Z. Pater, J. Tomczak, T. Bulzak, Numerical Analysis of Helical Rolling of a Hollow Roller Made of Titanium Alloy Ti6Al4V, Hutnik - Wiadomości Hutnicze **82** (9), 599-603 (2015).

[3] A. Kiełbus, D. Kuc, T. Rzychoń, Magnesium Alloys – Microstructure, Properties And Applications, Monograph Published on the Occasion of the 40th Anniversary of the Faculty of Materials Engineering and Metallurgy of the Silesian University of Technology in Katowice on "Modern Metallic Materials - the Present and the Future", Katowice (2009).

[4] I. Schindler, P. Kawulok, E. Hadasik, D. Kuc, Activation energy in hot forming and recrystallization models for magnesium alloy AZ31, Journal of materials engineering and performance **22** (3), 890-897 (2013).

[5] A. Kościelna, W. Szkliniarz, Titanium and its Alloys, Monograph Published on the Occasion of the 40th Anniversary of the Faculty of Materials Engineering and Metallurgy of the Silesian University of Technology in Katowice on "Modern Metallic Materials – the Present and the Future", Katowice (2009).

[6] A. Bylica, J. Sieniawski, Titanium and its Alloys, PWN, Warsaw (1985).

[7] A. Dziubińska, A. Gontarz, M. Dziubiński, M. Barszcz, The forming of magnesium alloy forgings for aircraft and automotive applications, Advances in Science and Technology Research Journal **10** (31), 158-168 (2016).

[8] O. Pashkowa, I. Ostrovsky, Y. Henn, Present state and future of magnesium application in aerospace industry, New Challenyes in Aeronautics, Moscow (2007).

[9] A.G. Beer, M.G. Barnett, Microstructure evolution in hot worked and annealed magnesium alloy AZ31, Material Science and Engineering **485**, 318-324 (2008).

[10] K.U. Kainer, Magnesium Alloys and Technologies, Wiley-VCH Verlag GmbH & Co. KGaA, Weinheim (2003).

[11] S. Rusz, L. Cizek, J. Kedron, S. Tylsar, M. Salajka, E. Hadasik, T. Donič, Structure and Mechanical Properties Selected Magnesium – Zirconium Alloys, Journal of Trends in the Development of Machinery and Associated Technology **16** (1), 55-58 (2012).

[12] F. Lv, F. Yang, Q.Q. Duan, Y.S. Yang, S.D. Wu, S.X. Li, Z.F. Zhang, Fatigue properties of rolled magnesium alloy (AZ31) sheet: Influence of specimen orientation, International Journal of Fatigue **33** (5), 672-682 (2011).

[13] J. Bohlen, D. Letzig, K.U. Kainer, New Perspectives for Wrought Magnesium Alloys, Materials Science Forum **546-549**, 1-10 (2007).

[14] J. Śleziona, M. Dyzia, J. Piątkowski, Aluminium and its Alloys, Monograph Published on the Occasion of the 40th Anniversary of the Faculty of Materials Engineering and Metallurgy of the Silesian University of Technology in Katowice on "Modern Metallic Materials – the Present and the Future", Katowice (2009).

[15] M. Cieśla, G. Junak, Low-cycle fatigue characteristics of 2017A aluminium alloy, AZ31 magnesium alloy and Ti-6Al-4V titanium alloy, METAL 2015, 24th International Conference on Metallurgy and Materials, Brno (2015).

[16] S. Kocańda, Fatigue Metal Cracking, WNT, Warsaw (1985).

[17] S. Kocańda, A. Kocańda, Low-Cycle Fatigue Strength of Metals, PWN, Warsaw (1989).

[18] J. Szala, Fatigue damage summation hypotheses, WUATR, Bydgoszcz (1998).